SUPPORTING INFORMATION for

Converting high modulus water-based elastomeric core-shell nanoparticle films from viscoelastic to predominantly elastic using di-epoxide crosslinking

Mollie Osborne-Richards[a],*, David Ring[b], Xuelian Wang[a], Sarah Wall[a], Steve Edmondson[a] and Brian R. Saunders[a],*

a) Department of Materials, University of Manchester, MECD(A), Manchester, M1 7HL, UK.

b) Synthomer (UK) Ltd, Temple Fields, Harlow, Essex, CM20 2BH, U.K

EXPERIMENTAL

Materials

Butyl acrylate (BA), sodium dodecyl sulphate (SDS, 98.5 %), potassium phosphate monobasic (KH_2PO_4, ≥ 99.0 %), ammonium persulphate (APS, 98 %) methacrylic acid (MAA, ≥ 99 %), acrylonitrile (AN, ≥ 99 %), 1,4-butanediol diacrylate (BDDA, ≥ 99 %), tertiary-dodecyl mercaptan (*t*-ddm, ≥ 99 %), 1,4-butandiol diglycidyl ether (BDDE, ≥ 65 %), butyl glycidyl ether (BGE, 95 %) were purchased from Aldrich and used as received. All water was de-ionized and of ultra-high purity.

Core-shell particle synthesis

The parent core-shell nanoparticles (denoted as CS-0) were prepared by a monomer-starved semi-batch emulsion polymerization using a method adapted from a microgel synthesis for the first time[1]. Water (258.8 g) containing SDS (0.90 g) and KH_2PO_4 (1.6 g of 7.0 wt.% solution) were added to a reaction vessel and degassed under N_2 for 20 min. The core was prepared by adding BA (40.0 g, 0.313 mol) to the reaction, followed by APS (5.0 g of 2.0 wt.% solution). The reaction mixture was stirred at 300 rpm under reflux for 60 min in a N_2 atmosphere at 80 °C. To prepare the shell, a co-monomer solution (80.06 g) containing BA (55.0 g, 0.40 mol), MAA (8. 0 g, 0.090 mol), AN (16.0 g, 0.302 mol), BDDA (1.16 g, 5.90 mmol) and *t*-ddm (0.020 g, 0.10 mmol) was prepared. This pre-emulsion was fed into the reaction at a rate of 0.90 mL min^{-1} over 90 min whilst stirring. Once the shell co-monomer solution had been completely added to the reaction it was then left to stir for a further 150 min. Finally, the latex was cooled to room temperature and filtered through an aluminium sieve (28 µm).

Stage I (*pre*-film casting) reaction of BDDE with the nanoparticles

A dispersion CS-0 (12.0 wt.%, 60.0 g) was prepared and adjusted to pH 5.0 using aqueous NaOH solution (< 1.0 mL, 0.25 M). To this dispersion, different masses of BDDE were added (0.25 g, 0.50, and 1.0 g) and the dispersion was then stirred for 6.0 h at 60 °C. These films are denoted as CS-*x*

where *x* = the mass of BDDE used in g.

Stage I (*pre*-film casting) reaction of BGE with the nanoparticles

A study using the monofunctional epoxide, BGE, was conducted using the same method as described for the addition of BDDE above. In this case BGE (1.0 g) was added, and the dispersion was then stirred for 6 h at 60 ˚C. 1.0 g of BGE gives an epoxy equivalent of approximately CS-0.7 (7.7 mmol).

Stage I + II film formation

A silicone mold (95 mm x 60 mm x 30 mm) was cleaned with soap, water, and acetone. The mold was then coated with Ambersil PTFE surface spray to make the silicone non-stick. A CS-*x* dispersion (12.0 wt.%, 20.0 g) that was subjected to the Stage I reaction (above) was poured into the mold which was then placed in a circulating oven at 30 °C for 48 h. These drying conditions were used for all films in this study. When the films were removed from the mold, they were measured to be approximately 500 μm thick with callipers.

Stage I (*pre*-casting) film formation via removal of unreacted BDDE

To study the effects of the Stage I reaction (Scheme 1) only on the film properties, unreacted BDDE was removed after the Stage I reaction was finished. After samples of CS-1 were reacted with BDDE during the Stage I reaction (described above), they underwent dialysis for 5 days with the water (250 g) being changed twice daily. This latex was then cast to produce films denoted as CS-1-D films. The process is depicted in Fig. 5a.

Stage II (*post*-casting) film formation with BDDE addition

To study the effect of the Stage II reaction (Scheme 1) only on the film properties, BDDE was added to CS-0 dispersion and the film casting process conducted. BDDE (0.33 g) was added to the CS-0 dispersion (12.0 wt.%, 20.0 g) which was then poured into a mold for film formation. This method produced films denoted as CS-0+BDDE and is depicted in Fig. 6a.

Physical Measurements

The concentration of MAA in the particles and the pK_a of the dispersions was determined by titration using a Mettler Toledo Easy Direct autotitrator and aqueous NaOH (0.10 M) solution. When $x = 0$, (i.e., CS-0) the amount of BDDE added is 0 g and the MAA content had the initial (maximum) value. From the latter value the BDDE content was calculated by measuring the absolute MAA concentration (in wt %) of each sample (CS-0.25, CS-0.5, and CS-1). Fourier transform infrared spectroscopy (FTIR) measurements were obtained using a Bruker alpha II instrument. Z-average particle diameter (d_z) and zeta potential (ζ) data were measured using a Zetasizer Nano ZS instrument; the d_z value was determined by the cumulant analysis method. For the zeta potential measurements, the samples were dispersed in aqueous NaCl solution (1.0 mM). The number of particles was determined by the following equation:

$$N_p = \frac{6m}{\pi \rho d_z^{\,3}}$$

(S1)

where m is the mass of the monomer that has been polymerised and ρ is the density of the copolymer (1.0 g cm^{-3}). The mass was determined with the aid of a gravimetric method by drying small (~1 g) samples of the dispersion at 80 °C for 24 h to obtain the total solids content. Scanning electron microscopy (SEM) images were obtained using the Tescan Mira3 Small Chamber instrument. The temperature-dependent mechanical properties were obtained from dynamic mechanical analysis (DMA) measured using a TA-Q800 in film tension mode with a frequency of 1 Hz. Each DMA sample measurement was replicated three times to determine a representative data set. The DMA provided tan δ (= E'' / E', where E'' and E' are the loss and storage moduli) data, from which the peak is assumed the T_g. These data allowed us to apply the Fox equation:

$$\frac{1}{T_g} = \frac{w_A}{T_{g(A)}} + \frac{w_B}{T_{g(B)}}$$

(S2)

where $T_{g(A)}$ and $T_{g(B)}$ are the glass transition temperatures of homopolymers A and B, respectively,

and w_A and w_B are the weight fractions of A and B in the copolymer. See Additional Note 2 for more detail. Thermal gravimetric analysis (TGA) was also conducted using a TA- Q500 in N_2 with a ramp of 10 °C min^{-1}. Uniaxial stress-strain measurements were obtained using an Instron 5564 mechanical testing system. The crosshead speed was 50 mm min^{-1} and films were stamped into dumbbell-shaped specimens with a length of 25 mm and a constricted width of 4 mm. The shear modulus (G) is taken from fitting the following equation to data measured over the 0 - 10 % strain range using the equation[2]

$$\sigma = G(\lambda - \lambda^{-2}) \tag{S3}$$

where σ is the stress and λ is the elongation ratio. Cyclic stress-strain measurements were measured at a rate of 50 mm min^{-1}. Each tensile measurement was replicated three times to determine a representative data set. Atomic force microscopy (AFM) imaging was conducted using a Multimode 8 in non-contact mode under ambient condition using a NuNano Scout 70 probe with a spring constant of 2 N/m and a resonant frequency of 70 kHz. The film mass swelling ratios were measured by immersing pre-weighed films in solvents for five days and then weighing the swollen films, drying and weighing again. The mass swelling ratios for the films were calculated using the equation:

$$Swelling\ ratio = \left(\frac{m_1}{m_2}\right) \times 100 \tag{S4}$$

where m_1 is the swollen weight and m_2 is the weight after the film has dried in air for 24 h.

Additional note 1: Core-shell nanoparticle synthesis

Core-shell nanoparticles were synthesized by semi-batch emulsion polymerization and produced poly(butyl acrylate)/poly(butyl acrylate-*co*-acrylonitrile-*co*-methacrylic acid-*co*-1,4-butanediol diacrylate) (PBA/(PBA-AN-MAA-BDDA)) nanoparticles (denoted at CS-0) as shown in Scheme S1. The core was prepared and then a feed of the shell monomers was added into the reaction to give the core-shell nanoparticles as described above.[3] The *z*-average diameter (d_z) data in Fig. S1a show the core has an initial measured diameter of 70 nm and with the addition of the shell the particles grow to approximately 100 nm. Whilst there is scatter in the data, the number of nanoparticles (N_p) remains constant which suggests no secondary nucleation occurred (Fig. S1b).
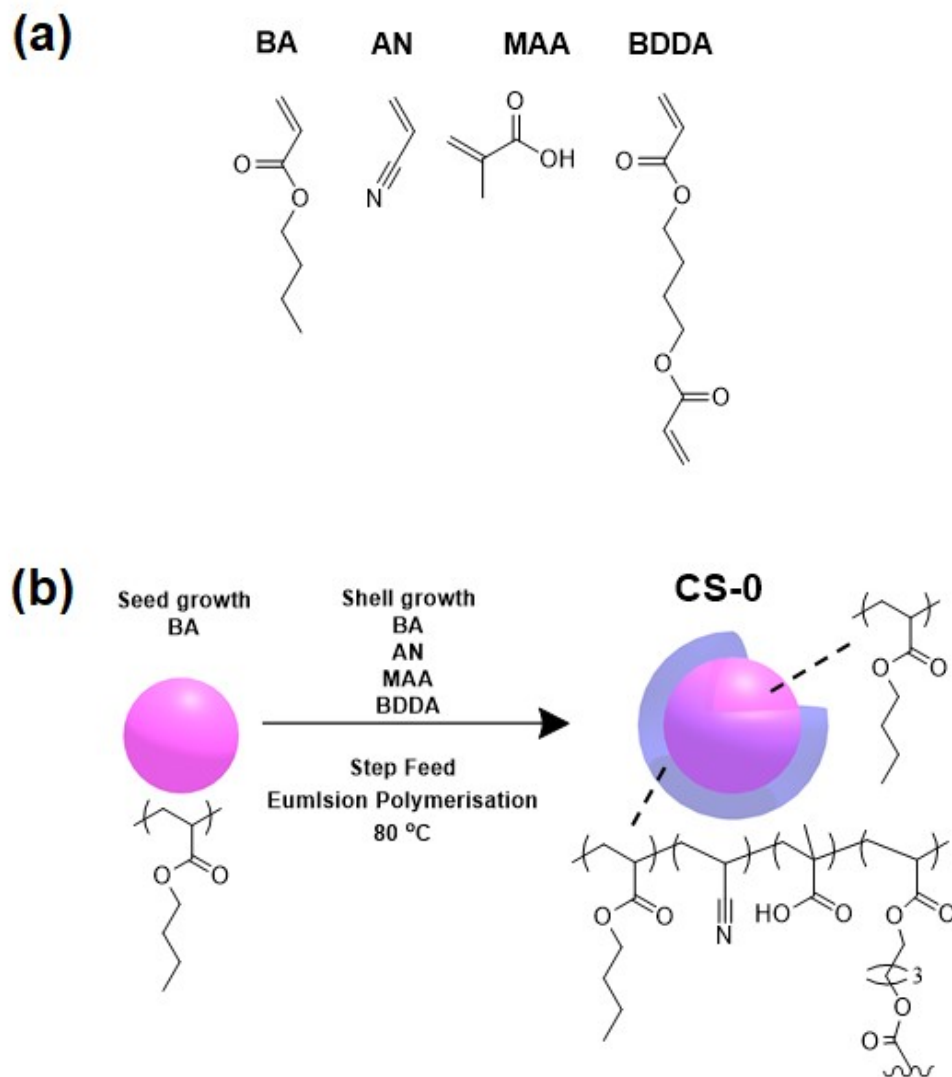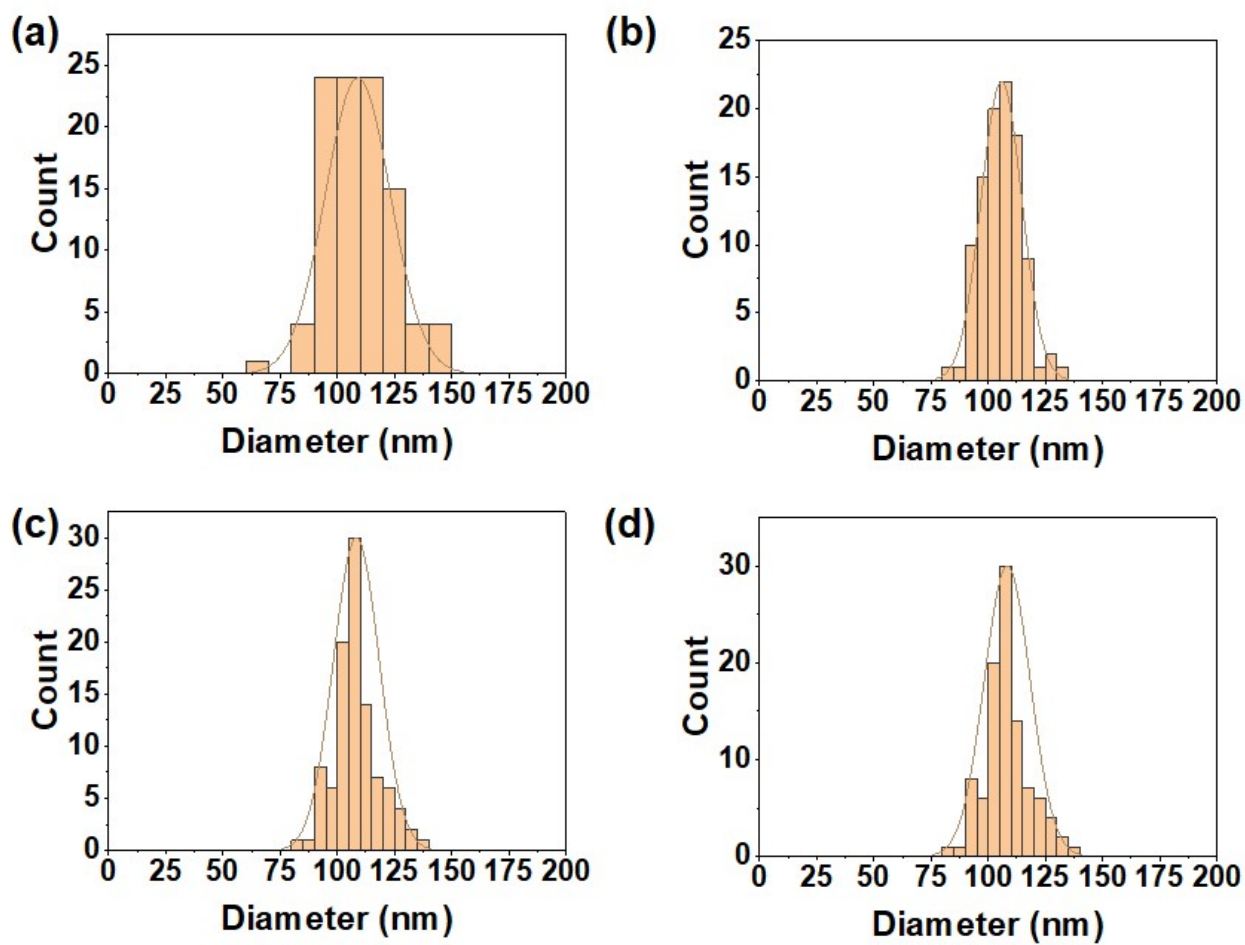
Scheme S1. (a) Structures of the monomers and **(b)** depiction of the synthesis for the PBA/(PBA-AN-MAA-BDDA) (CS-0) nanoparticles.
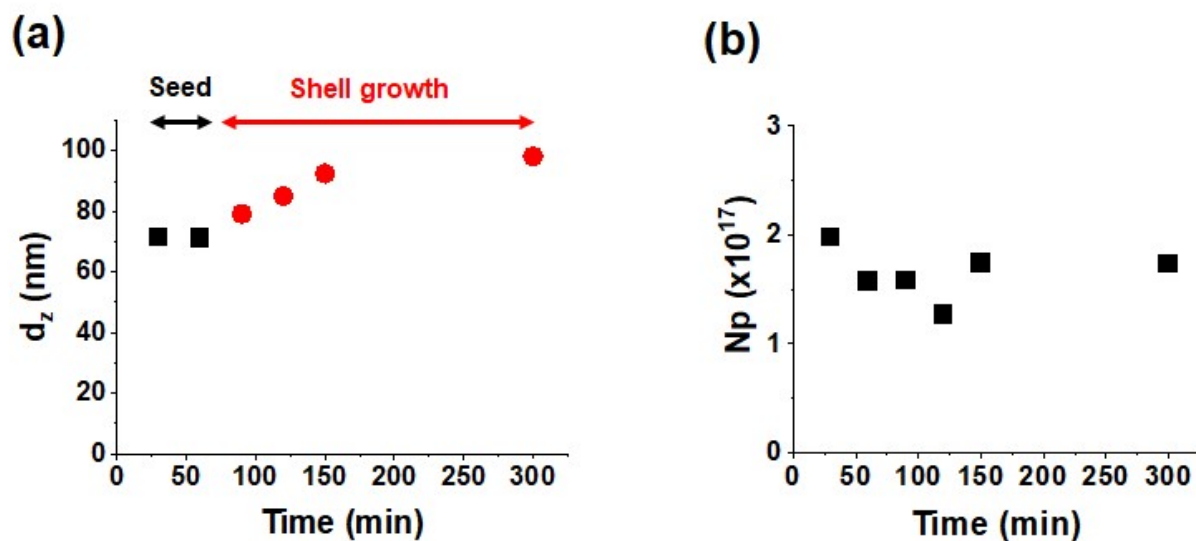
Fig. S1. Variation of **(a)** z-average diameter of particles during the synthesis of CS-0. **(b)** Calculated number of particles over the course of particle growth.

Fig. S2. Size distributions of **(a)** CS-0, **(b)** CS-0.25, **(c)** CS-0.5 and **(d)** CS-1 nanoparticles from the SEM images shown in Fig. 1a-1d.
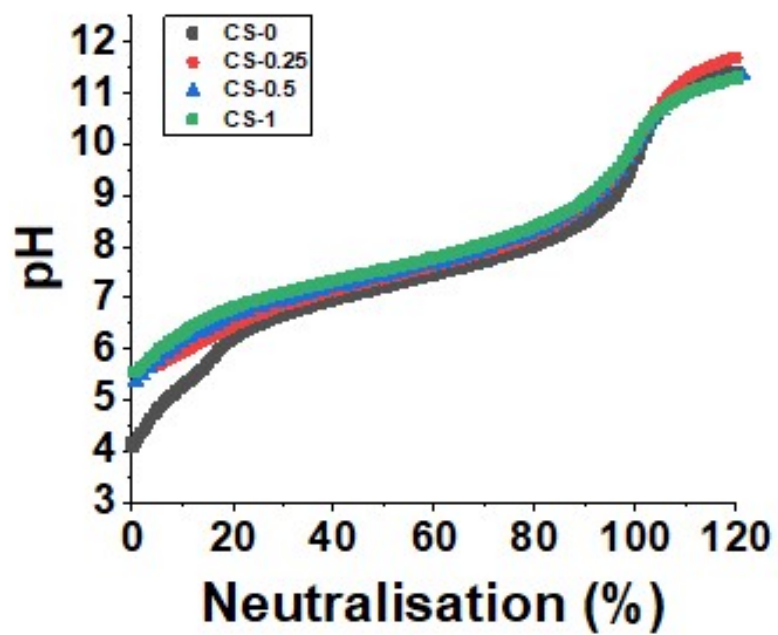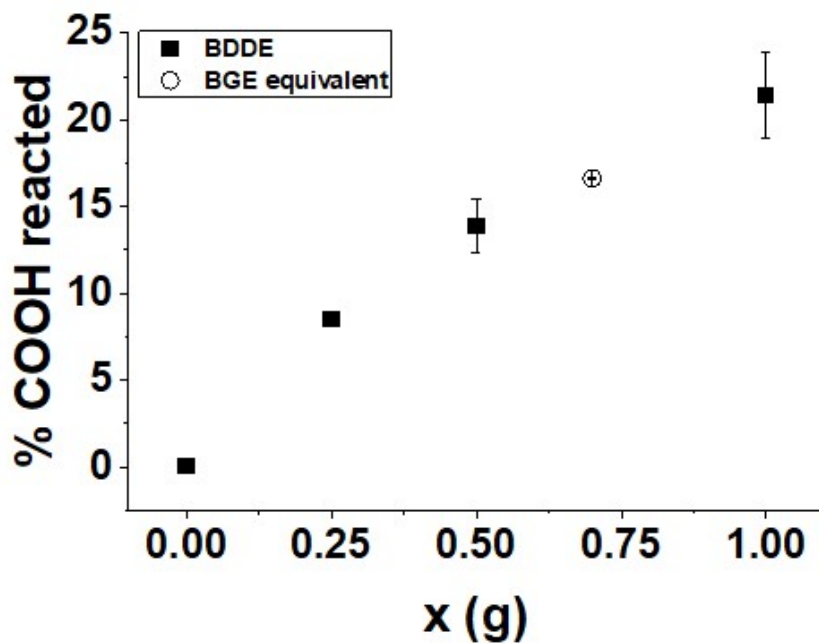
Fig. S3. Potentiometric titration curves measured for the CS-*x* dispersions.

Fig. S4. Estimated percentage of the initial -COOH groups in the CS-*x* nanoparticles that had reacted as a function of the mass of the BDDE mass initially added at the *pre*-film casting stage (Stage I). The BGE equivalent data point refers to later in this study (Additional Note 3) where BGE is used in place of BDDE. A hypothetical BDDE equivalent mass of 0.70 g would need to be used to achieve the same number of moles of epoxide groups as those added for the BGE system.
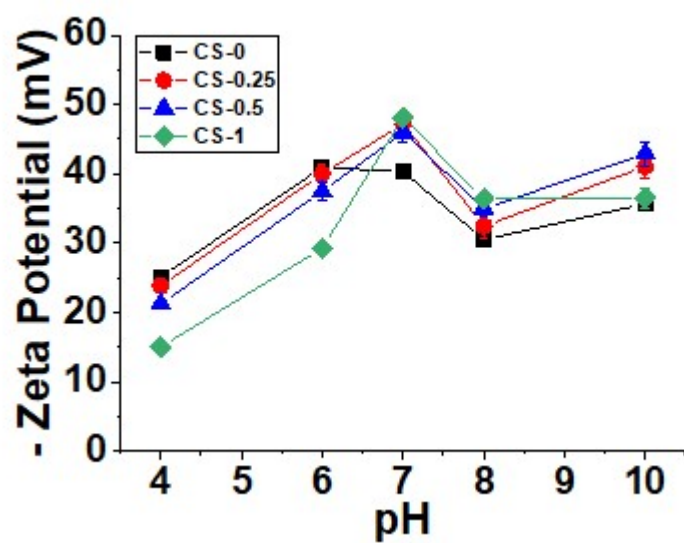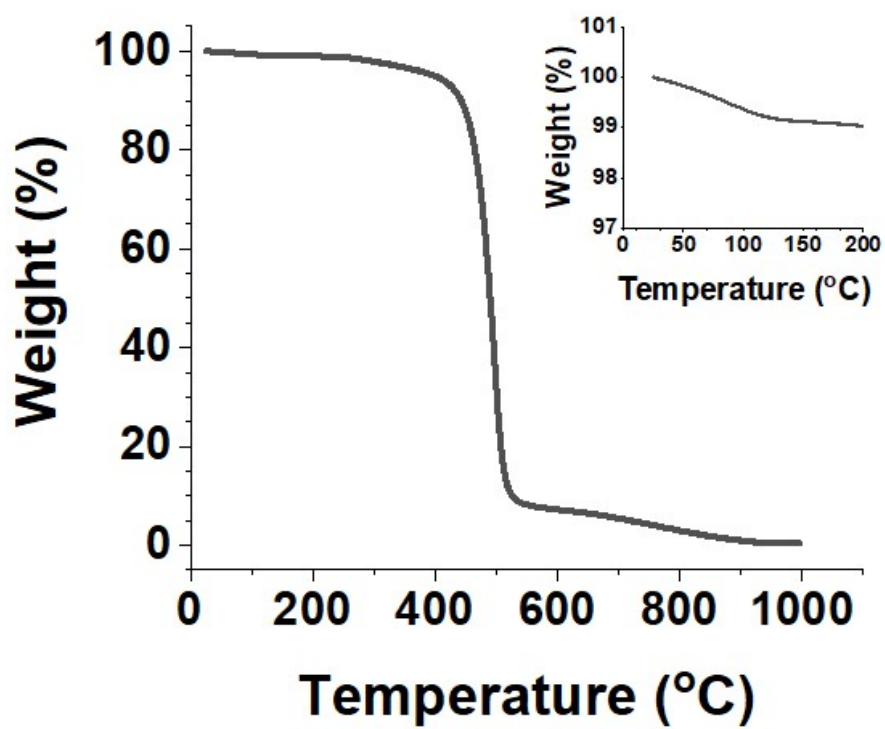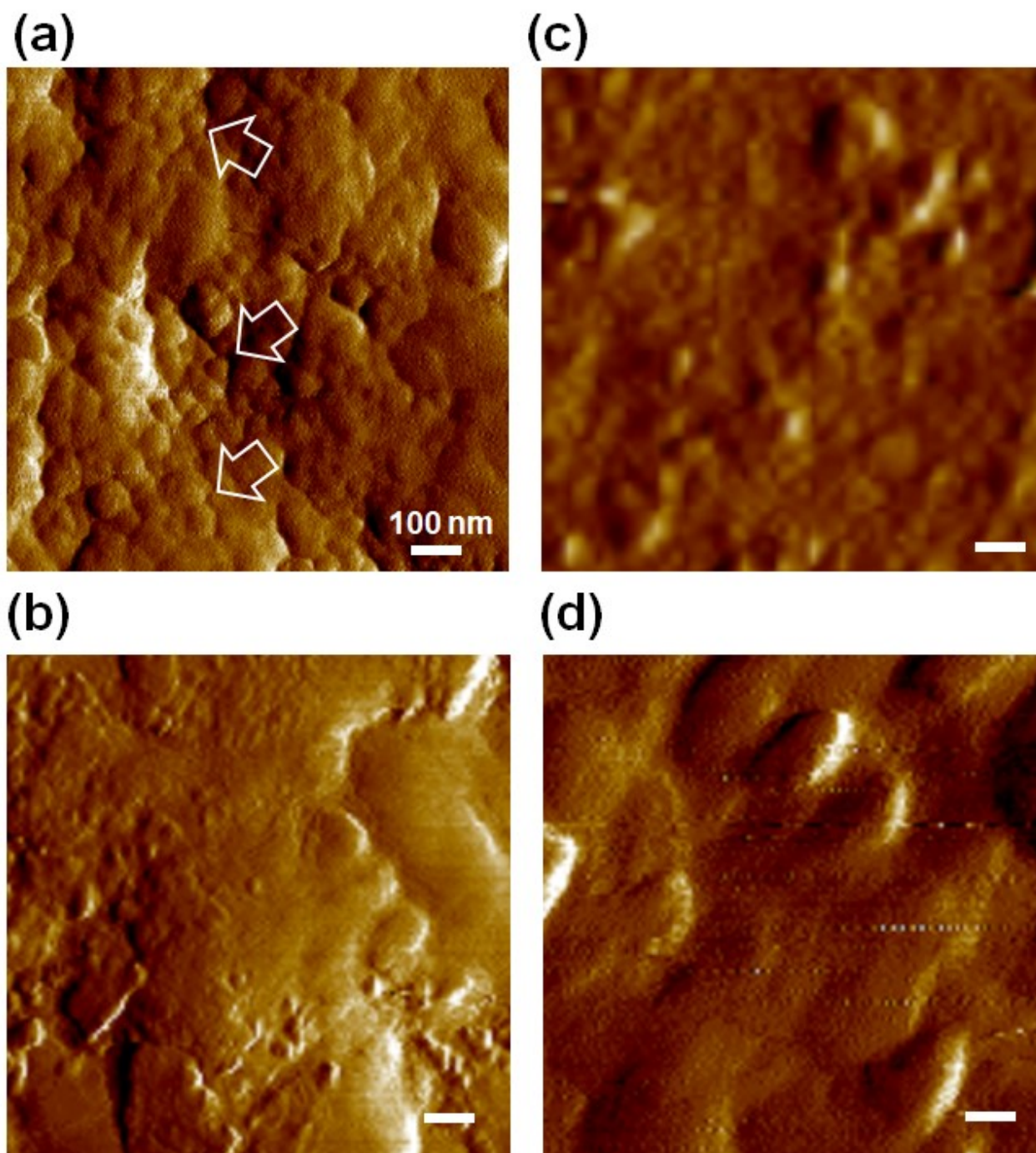
Fig. S5. The zeta-potential of the CS-*x* nanoparticles when dispersed in different pH solutions.

Fig. S6. TGA analysis of a CS-0.5 polymer film. The inset shows an expanded view.

Fig. S7. AFM peak force error mode scans of the **(a)** CS-0, **(b)** CS-0.25, **(c)** CS-0.5 and **(d)** CS-1 films. The arrows in (a) highlight well-defined CS-0 nanoparticles. The nanoparticles have coalesced in (b) to (d) and are not individually distinguishable. The scale bars are 100 nm.
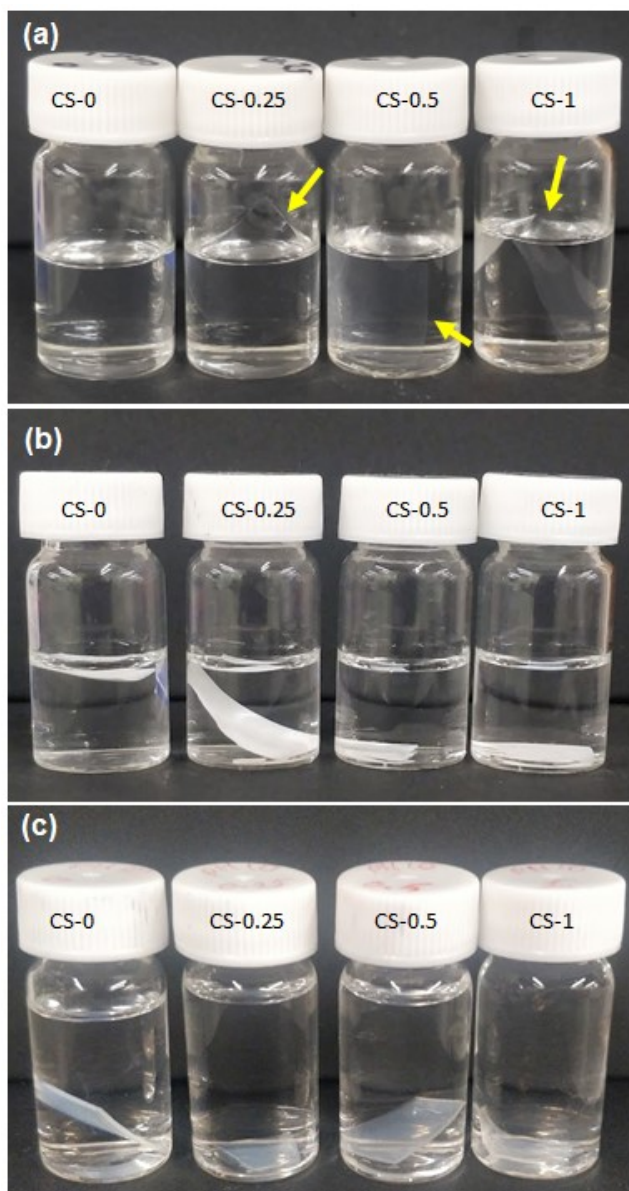
Fig. S8. Photographs of the CS-*x* films in **(a)** CHCl$_3$, **(b)** water at pH 6 and **(c)** water at pH 10. All photographs were obtained after the films had equilibrated in the solvent for 5 days. The CS-0 film in (a) swelled so strongly that it became brittle and disintegrated when attempts were made to measure the swollen mass. The arrows in (a) highlight the films.
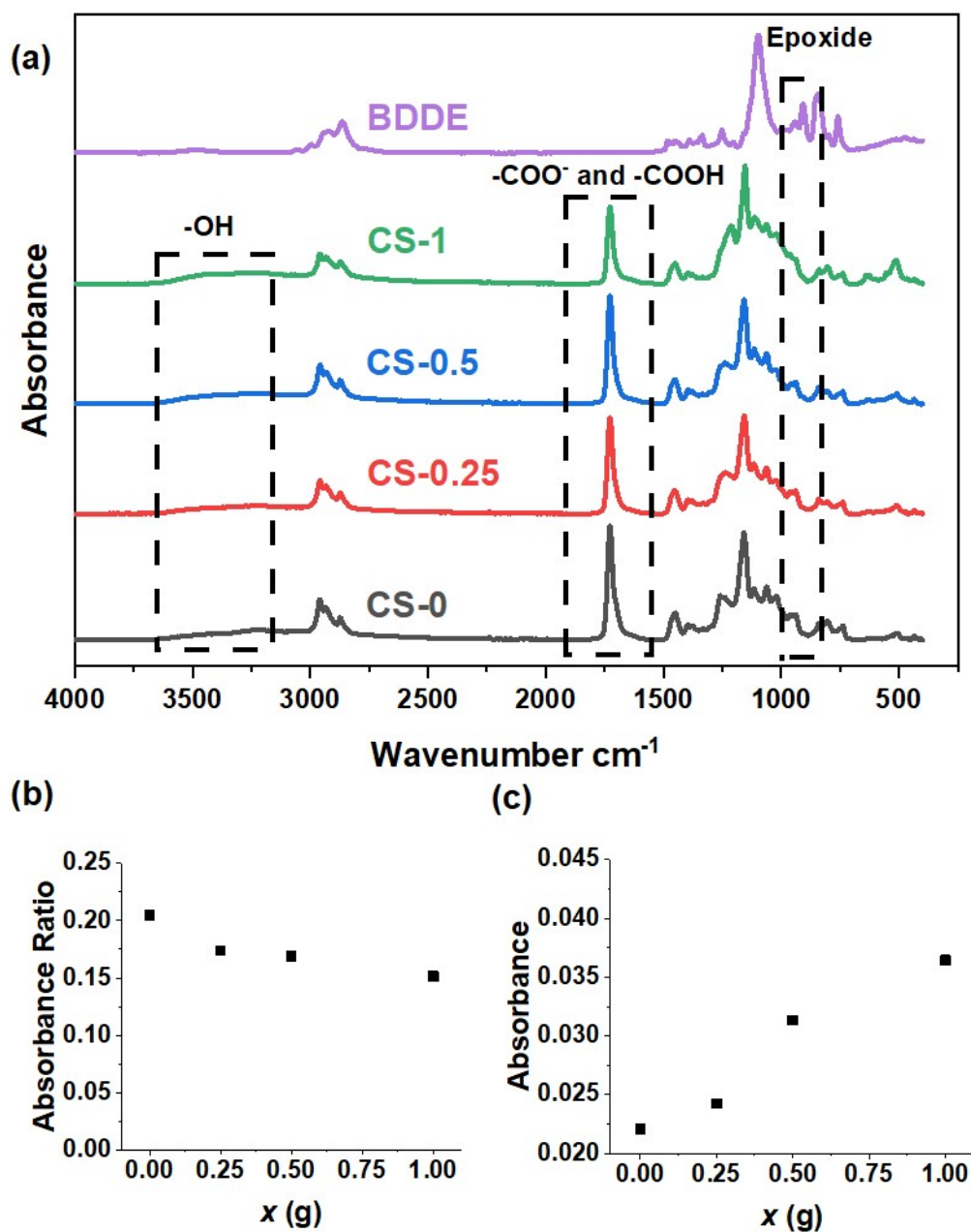
Fig. S9. (a) FTIR spectra of the CS-*x* films. The regions highlighted are expanded and shown in Fig. 2d – 2f. **(b)** Absorbance ratio of the -COOH peak at 1700 cm^{-1} to the sum of the absorbances at 1700 and 1730 cm^{-1} (due to ester groups). **(c)** Absorbance of the -OH peak at 3500 cm^{-1} due to -OH formation (from reaction of –COOH with epoxide) measured for each film.

Additional note 2: The Fox equation

We applied the Fox equation for predicting poly(A-*co*-B) copolymer glass transition values to our systems.[2] It is understood that the Fox equation applies to a copolymer containing two types of monomers that are randomly distributed along the copolymer chain and that the T_g values of the respective poly(A) and poly(B) homopolymers are different. In contrast the present systems consist of core-shell nanoparticles with every particle having the same composition as its neighbour for a given value of *x*. By applying the Fox equation to the present systems we are testing whether a blending law for polymers comprised of linear copolymer chains can be applied to core-shell nanoparticle films where changes in the shell composition control the overall nanoparticle film T_g. Here, we assume that when we have a value of *x* between 0 and 1.0 we have a copolymer system of CS-0 (*x* = 0) and CS-1 (*x* = 1) where *x* is the measure of the weight (mass) fraction of *x* = 1 within the copolymer blend of CS-0 and CS-1. This assumption enabled calculation of theoretical T_g values for CS-0.25 and CS-0.5 based on the value for *x*. According to Equation S2 we took $T_{g(A)}$ to be that of CS-0 (i.e., 66.0 °C) and $T_{g(B)}$ to be that of CS-1 (i.e., 8.7 °C) and calculated the theoretical T_g values for the CS-0.25 film (using $w_A = 0.75$) and CS-0.5 film (using $w_B = 0.5$). The results are shown in Fig. 3c. Fortuitously, the values for *x* had the same numerical values as w_B in this study.

**Additional Note 3: Evidence for di-epoxide crosslinking in the films**

To confirm that the BDDE acted as a crosslinker we replaced BDDE with a mono-epoxy species (BGE, Scheme S2). We denote this CS-0 nanoparticle with added BGE as CS-0-BGE. Films were prepared using the Stage I + II method and had the equivalent number of epoxy groups to CS-0.7. Indeed, the titration data for this system (Fig. S10a and Table S1) when plotted in terms of %COOH reacted and an equivalent mass to a hypothetical CS-0.7 system (i.e., $x = 0.7$ in Fig. S4) show very good agreement with the CS-x BDDE-containing systems. These data indicate that there was no difference to the RCOOH reaction efficiency when BDDE or BGE was used. Accordingly, CS-0-BGE is compared to both CS-0.5 and CS-1. Variable pH DLS data (Fig. S10b) show a slightly decreased d_z compared to CS-0.5 at higher pH, which indicates that the mono epoxy ring reacted with some of the RCOOH groups available which decreased the concentration of -COO$^-$ groups at high pH. After reaction with BGE, the nanoparticle diameter has not changed in size, similar to the reaction of BDDE with the nanoparticle. The nanoparticle number-average diameter (111 nm) apparent from Fig. S11a and S11b is not dissimilar to the BDDE functionalised nanoparticles shown in Fig. 1a - 1d. Swelling data for a CS-0-BGE film in CHCl$_3$ gave a mass swelling ratio of 620 % (Fig. S12). The latter is larger than the swelling ratio for the CS-0.5 film (562 %, Fig. 2c). Moreover, this film was exceptionally fragile in the swollen state indicating a lack of crosslinking.
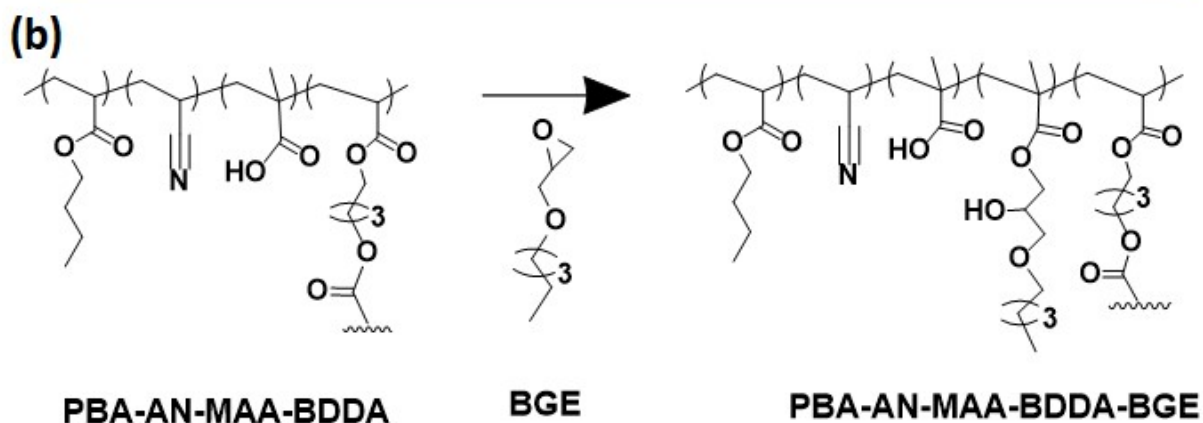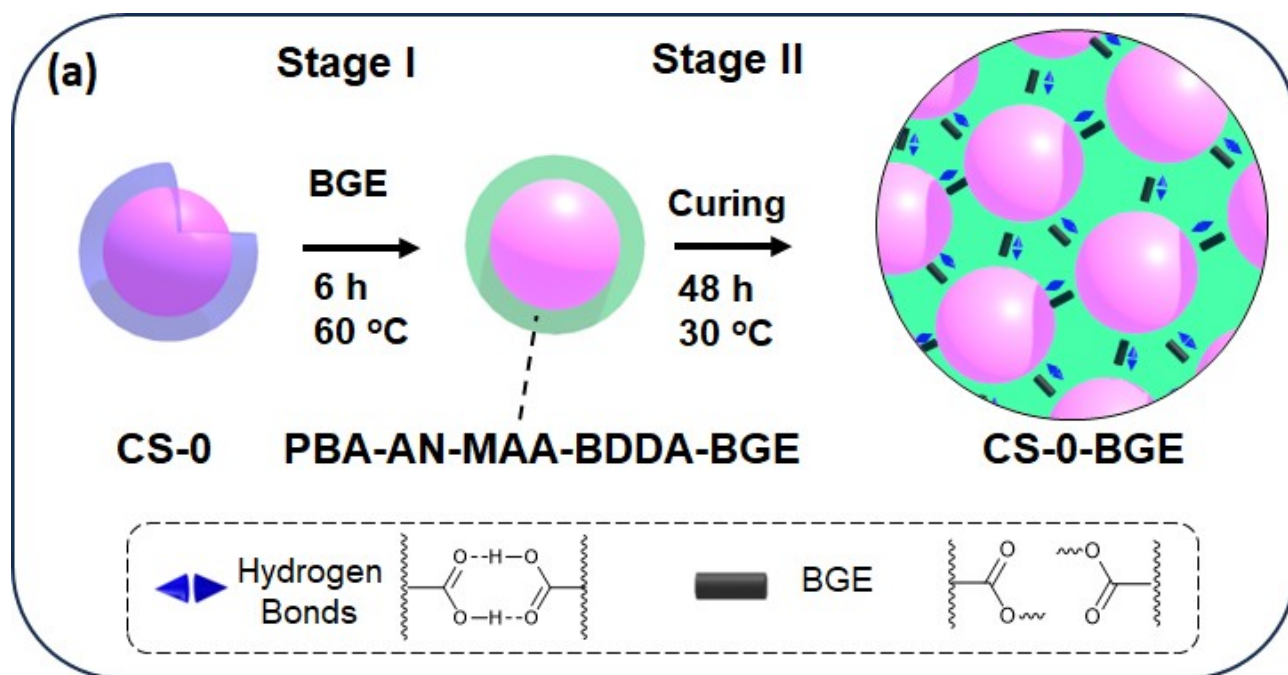
Scheme S2. (a) Depiction of the formation of CS-0-BGE films (butyl glycidyl ether) after the first *pre*-film casting reaction (Stage I) followed by the *post*-casting reaction during film formation (Stage II). Stages I and II indicate the stages of reaction of BGE with the -COOH functional groups of the particles. **(b)** Reaction scheme of BGE reacting with some of the -COOH groups within PBA-AN-MAA-BDDA.
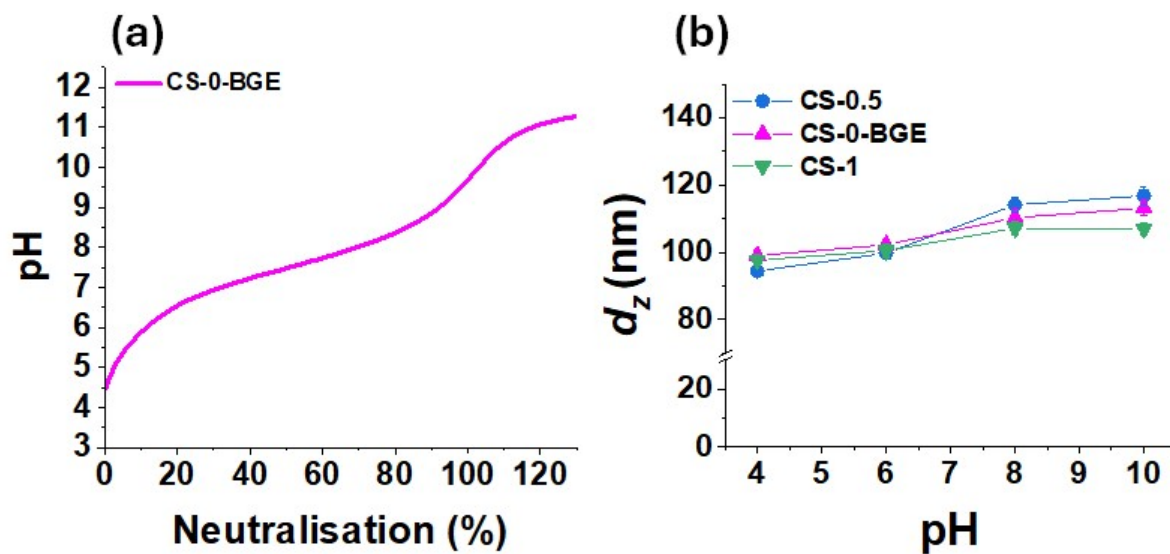
Fig. S10. (a) Potentiometric titration curve measured for the CS-0-BGE dispersion. **(b)** Comparison of how the CS-0.5, CS-1 and CS-0-BGE particles swell as the pH is increased.
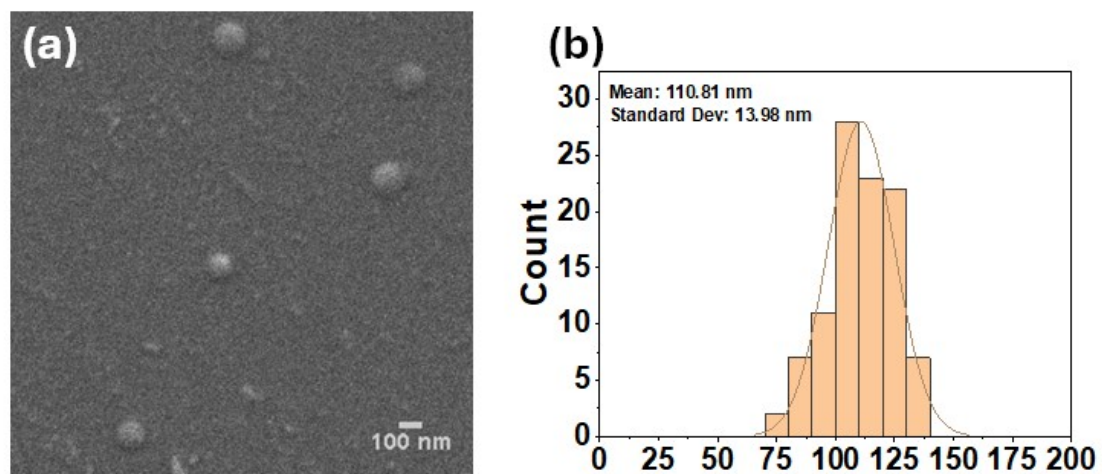
**Fig. S11. (a)** SEM of CS-0 -BGE particles, scale bar is 100 nm. **(b)** Size distribution of CS-0 -BGE nanoparticles.
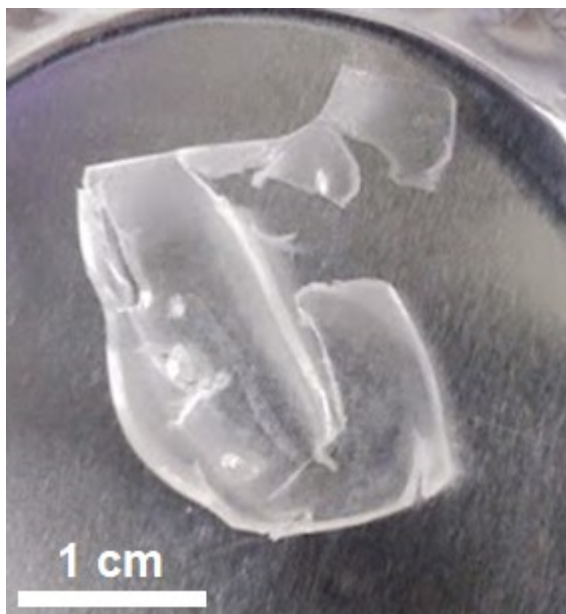
Fig. S12. Image of the swollen CS-0-BGE film after 5 days in a CHCl$_3$; it was very brittle and broke apart as it was weighed.

The DMA data measured for CS-0-BGE (Fig. S13a) gave a T_g of the film is 45 °C which is a little higher than that for CS-0.5 (36 °C, Fig. 3c), and considerably higher than CS-1 (9 °C). These data support the view that the ring-opening reaction of epoxide with -COOH reaction (and the decrease in -COOH concentration) is responsible for the T_g decrease for the CS-0-BGE film. The tensile data for this system (Fig. S13b) are much higher than CS-0.5 and CS-1 as can be seen for the shear modulus (Fig. S13c) and stress-at-break (Fig. S13d), and strain-at-break (Fig. S13e) data. The titration data indicate that there was no difference to the -COOH reaction efficiency between BDDE and BGE which suggests that the reason for the change in mechanical properties is differences between how BDDE and BGE react within the shells. We speculate that differences for the mechanical properties are because of the spatial differences in the locations of the BDDE and BGE reactions. For the former two epoxide groups must react at sites that are within a monomer length of each other (~ 1.3 nm based on the BDDE structure). Such co-located reactions should lock chains in their relative positions and oppose rearrangement that would give close approach of multiple neighbouring -COOH groups. In contrast, two BGE molecules (and the two epoxide groups) do not have to co-react in the same location and the reaction with BGE occurs more uniformly throughout the nanoparticle shell, allowing tighter chain packing and more restricted free volume in the shell. Such an arrangement should lead to a more organised -COOH-based hydrogen bonding, increasing the shear modulus, strain-at-break and stress-at-break for the CS-0-BGE films.
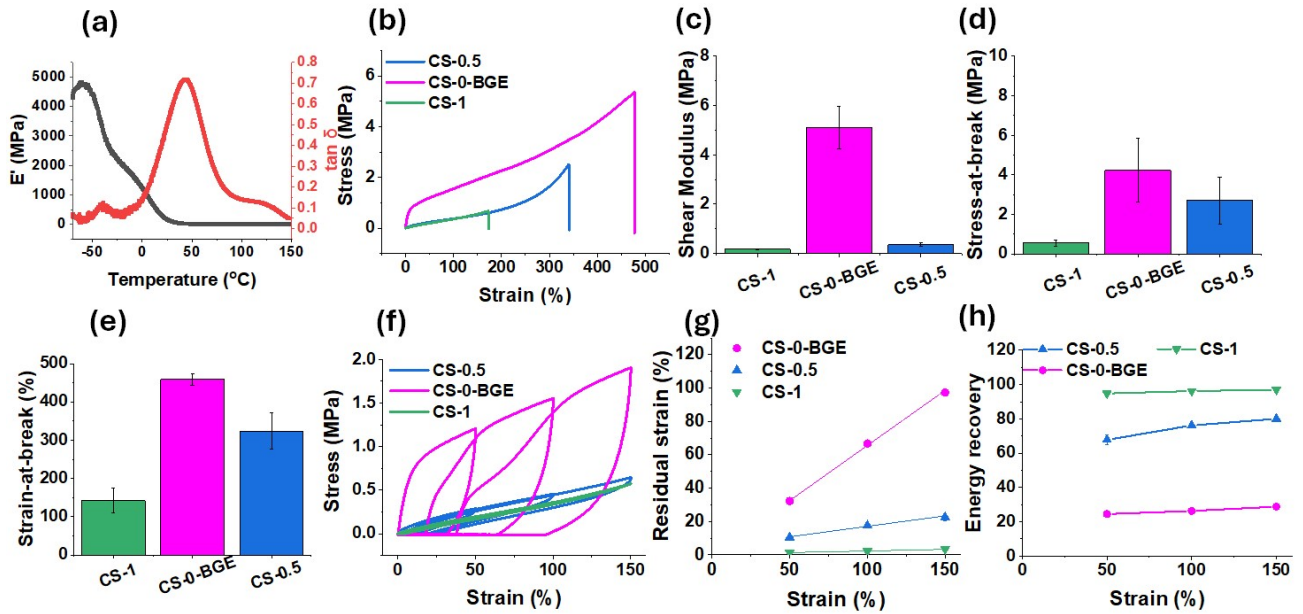
Fig. S13. (a) Representative variation of *E'* and tan *δ* with temperature measured for the CS-0-BGE film. **(b)** Representative stress-strain curve of CS-0-BGE compared to CS-0.5 and CS-1. The representative **(c)** shear modulus, **(d)** stress-at-break and **(e)** strain-at-break values are shown. **(f)** Representative cyclic tensile stress-strain data for CS-0-BGE. Data for CS-0.5 and CS-1 are shown for comparison. Residual strain and energy recovery at various strains are shown in **(g)** and **(h)**, respectively.

Cyclic tensile data (Fig. S13f) were also measured. CS-0-BGE residual strain (Fig. S13g) and energy recovery (Fig. S13h) do not compare to the residual strain and energy recovery of CS-0.5 or CS-1. Indeed, the CS-0-BGE residual strain is much higher and the energy recovery much lower than those measured for the CS-0.5 and CS-1 films. These data show the CS-0-BGE film has poor elastic properties and is a dissipative film. This confirms that no covalent crosslinking occurred when BGE was used. We can use these data for BGE to make inferences about BDDE as a crosslinker. It follows that if BDDE was only reacting at one end (monofunctional reaction) the cyclic tensile response would be similar to CS-0-BGE. Therefore, it is highly likely that the BDDE reacted at both ends, (bi-functional reaction) i.e., producing covalent crosslinking.

Table S1. The size and measured acid content for each nanoparticle dispersion studied.

	d_{SEM} (nm)	d_z (nm)^a	MAA (wt%)	pK_a
CS-0	109 ± 14	102 ± 2.4	8.91 ± 0.07	7.2
CS-0.25	108 ± 10	98 ± 0.4	8.15 ± 0.32	7.4
CS-0.5	108 ± 10	100 ± 2.0	7.67 ± 0.85	7.4
CS-1	106 ± 9	101 ± 2.2	7.00 ± 0.81	7.6
CS-0-BGE	110 ± 14	102 ± 1.8	7.43 ± 0.01	7.4

^{a} Measured at pH 4.

Table S2. Tensile data for the films studied.

	Shear modulus (MPa)	Strain-at-break (%)	Stress-at-break (MPa)
CS-0	9.0 ± 0.8	343 ± 19	8.0 ± 0.5
CS-0.25	1.1 ± 0.06	379 ± 5	5.0 ± 0.4
CS-0.5	0.40 ± 0.07	323 ± 47	3.0 ± 1
CS-1	0.20 ± 0.01	142 ± 31	0.6 ± 0.2
CS-1-D	5.0 ± 1.0	318 ± 54	6.0 ± 2
CS-0+BDDE	3.7 ± 0.4	436 ± 8	7.0 ± 0.4
CS-0-BGE	5.0 ± 0.9	459 ± 16	5.0 ± 2

References

1. B. E. Rodriguez, M. S. Wolfe and M. Fryd, *Macromolecules*, 1994, **27**, 6642.
2. P. J. Flory, *Principles of Polymer Chemistry*, Cornell University Press, USA, 1953.
3. J. Turton, S. Worral, M. S. Musa, A. H. Milani, Y. Yao, P. Shaw, D. Ring and B. R. Saunders, *Polym. Chem*, 2021, **12**, 466.